A Mid and Far Infrared View of Galaxies

C. J. Cesarsky (ccesarsk@eso.org)
C.E.A. Saclay, DSM/DAPNIA/Service d'Astrophysique, 91191 Gif sur Yvette Cedex, FRANCE
European Southern Observatory, Karl-Schwarzschildstr. 2, D-85754 Garching bei München, GERMANY

M. Sauvage (msauvage@cea.fr)
C.E.A. Saclay, DSM/DAPNIA/Service d'Astrophysique, 91191 Gif sur Yvette Cedex, FRANCE

Abstract. From the disk of normal galaxies to the nucleus of prototype active sources, we review the wealth of results and new understanding provided by recent infrared probes and, in particular, the four instruments on-board of *ISO*.

Keywords: infrared: lines and bands – infrared: continuum – galaxies: active – galaxies: starburst – stars: formation – ISM: infrared

1. Introduction: infrared emission processes

By allowing us a detailed view of the full 2-200 μm spectral range, *ISO* has dramatically increased our ability to investigate the processes giving rise to the spectral energy distribution (SED) of galaxies. Yet before actually starting this review, let us use well-known Galactic sources to exemplify the links between SEDs and the physical state of the objects in which they occur.

1.1. Mid-infrared bands and transient heating

The mid-infrared (MIR, 5-40 μm) is distinct from the far-infrared (FIR) in the sense that it shows a large number of broad spectral bands (especially in the 5-15 μm range) and that most of the dust is out of thermal equilibrium, in a regime of transient heating. The interesting property of transient heating is that, for a range of energy densities, the MIR flux scales linearly with the heating flux. This is clearly shown by Boulanger et al. (1998a) where they compare the MIR spectrum obtained on the peak of the NGC 7023 region (exposed to a B star radiation field) to that obtained on a diffuse cloud in the Chameleon region: the radiation fields differ by more than 3 orders of magnitude yet the MIR spectra are virtually identical. More quantitatively, they have shown that this linear scaling remains valid for radiation fields lower than a few 10^3 times the solar neighborhood value.

Without expanding on the nature of the dust giving rise to this family of bands, it is worthwhile to list a few properties that *ISO* has now firmly established. Even at the high resolution of the *ISOSWS*, the bands do not break up into a family of lines (as suggested e.g. by Léger et al., 1989). In fact, in most regions of the ISM, the band profiles are very constant, and much better represented by Lorentzian than by Gaussian functions (see e.g. Boulanger et al., 1998b; Mattila et al., 1999). Given the broad wings of a Lorentzian, in regions where the bands are prominent, most of the detected flux actually comes from the band carriers. As the debate still continues on the exact nature of the carriers, we will refer to them as the "infrared bands".

Studies of Galactic regions also help to pinpoint the major sites of emission: although they are detected in diffuse cirrus clouds (Boulanger et al., 1996), most of the infrared band emission originates in the interface between HII regions and molecular clouds, the photo-dissociation regions (PDR, see e.g. Cesarsky et al., 1996; Verstraete et al., 1996).

1.2. Continuum emission

From 10-15 μm to the submillimeter, the SEDs of most sources consist of a broad continuum. This continuum cannot be fitted by a single back-body curve. On the long wavelength side, this is due to the existence of more than one component of dust in thermal equilibrium. On the short wavelength side, this is due to the transition from the transient heating regime to the thermal equilibrium regime: below a size threshold fixed by grain properties and the radiation field intensity, dust grains still undergo noticeable temperature fluctuations. Depending on the heating radiation field, continuum emission will start to dominate over the infrared bands in the 12-15 μm range (e.g. in the PDR of M 17-SW, Cesarsky et al., 1996), or even over the whole MIR range (e.g. in the HII region of M 17-SW, Cesarsky et al., 1996, see also the evolution of compact HII region spectra in Cox et al., 1999). One should note however that except in regions with a particularly hard radiation field, the MIR spectrum is generally dominated by the infrared bands.

1.3. infrared lines

The IR domain also gives access to very important diagnostic lines. These allow an almost extinction-free measurement of the intrinsic ionizing spectrum, the nature of the energy source, or the energetics of the interstellar medium (e.g. through the [CII] 158 μm or [OI] 63 μm lines).

The great advantage of ISO in this area is the possibility to observe the full set of lines from an object, free of any foreground emission, in a single fixed aperture (see e.g Colbert et al., 1999, for M 82).

1.4. Active sources

The three previous sections referred to emission processes occurring in the interstellar medium (ISM) of galaxies. However, the IR is also a wavelength range where emission from active galactic nuclei (AGN) can be detected. This can take two forms: (1) thermal emission from dust in the torus around the AGN, in which case we expect a very hot continuum as grains probably reach their sublimation temperatures, and (2) synchrotron emission from charged particles in the AGN strong magnetic field, in which case the emission takes the form of a featureless spectrum increasing with frequency.

2. The interstellar medium in galactic disks

A great deal of attention has been devoted to the characterization of nearby spirals' IR emission. This has led to a deeper understanding of the distribution of dust in galaxies.

2.1. Cold dust and the total amount of dust

Assuming that the *IRAS* 60 and 100 μm fluxes from galaxies sample a single dust phase, dust masses and temperatures have been computed. Typical dust temperatures of $\sim$30 K and dust masses one order of magnitude below that deduced for the Milky Way were obtained (e.g. Devereux & Young, 1990). The advent of millimeter bolometers showed that this was likely an artifact of the wavelength domain sampled by *IRAS*, but uncertainties in the exponent of the emissivity in the FIR/mm range prevented a definitive assessment of the question.

With the combination of *ISO* and *SCUBA*, this is now being resolved. The full FIR/mm SEDs of nearby spiral galaxies reveal a consistent picture: in normal galaxies (i.e. star-forming but not starbursting spirals) most of the emission longward of 150-200 μm is provided by a cold dust phase (T$\simeq$10-20 K, Alton et al., 1998a; Bianchi et al., 1998; Davies et al., 1999; Haas et al., 1998; Israel et al., 1999; Krügel et al., 1998). In fact, Alton et al. (1998a) show clearly that the cold dust emission provides a significant fraction of the 100 μm flux. This mixed nature of the 100 μm *IRAS* band is very likely at the origin of numerous controversies on the interpretation of *IRAS* luminosities. Dust masses measurements now yield gas-to-dust ratios in external galaxies in the range 100-300, much more in agreement with the value of $\sim$160 measured in our galaxy.

These studies also point to a FIR/mm emissivity index of 2 (i.e. β in $\kappa_\nu \propto \nu^\beta$) rather than the more commonly used 1.5 .

2.2. Spatial distribution of the IR emission

Although all infrared maps show similar features, i.e. enhanced emission in the spiral arms and nucleus, a number of properties are emerging. Alton et al. (1998b) and Davies et al. (1999) have shown that *ISOPHOT* 200$\,\mu$m maps of normal spirals have a scale-length which is as large, or even larger than that of the stars. As the dust temperature probably decreases outwards, this implies that the scale-length of the cold dust column density is even larger. Comparison of radial profiles between cold dust traced at 850$\,\mu$m with *SCUBA* and the atomic and molecular components show that while the cold dust is more extended than the molecular gas, it is still less extended than the HI gas (Davies et al., 1999). Furthermore the radial distributions of dust and molecular gas agree well in the central part of the disk (Israel et al., 1999). This suggests that this cold dust is mostly associated with the molecular gas but that a non-negligible fraction also resides in the HI gas. As we progress outward in the galaxy, the ISM becomes mostly atomic and the dust phase associated to HI becomes more apparent.

Warmer dust, such as that detected by *IRAS* or *ISOCAM*, is clearly less extended than the cold phase and has a scale length smaller than that of the stars. In NGC 6946, Malhotra et al. (1996) have shown that the *ISOCAM* profiles at 6.75 and 15$\,\mu$m have a scale length similar to that of the molecular gas and Hα emission. The 60$\,\mu$m scale length is intermediate between that of molecular gas and stars. In fact it is close to that of the HI+H_2 profiles, likely showing a transition between the warm and cold component. In a thorough *ISOCAM* study of the SW ring in M 31, Pagani et al. (1999) show a clear spatial correlation of the MIR emission with HI and H_2, while the correlation is much poorer with Hα. This effect is also seen in NGC 891 (Mattila et al., 1999) and NGC 7331 (Smith et al., 1998).

The association of the MIR radiation with the HI+H_2 gas in the inner part of the galaxies confirms that the emission originates mainly from the PDRs at the outer layers of interstellar clouds. Instead, the larger scale-length of the FIR/mm component points, for the colder dust, to an origin in the inner parts of interstellar clouds.

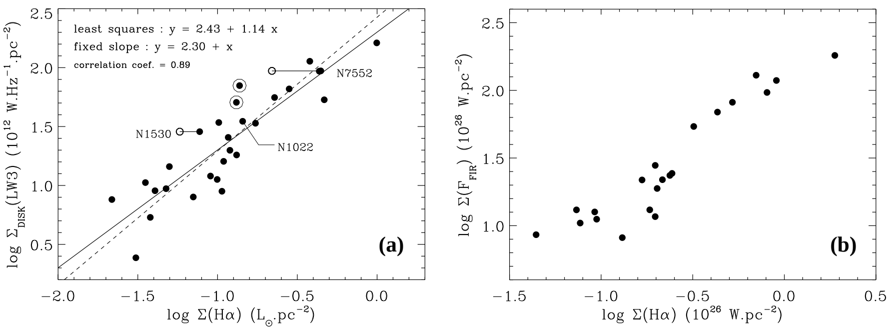

Figure 1. (a-left) The linear correlation between the 15 μm and Hα luminosities in the disk of spiral galaxies (normalized by the disk's surface to cancel scale effects). A similar linear correlation is observed with 6.75 μm luminosities. (b-right) The correlation between the FIR and Hα *total* fluxes for galaxies that have little contribution of the central regions in the 15 μm maps. On this sample, the correlation is linear, revealing a tight link between the two quantities (figures adapted from Roussel et al., 1999b).

2.3. Heating sources

A long standing question has been the heating source for the IR emission, and in particular, the extent to which this emission can be considered a good star formation tracer (see e.g. Kennicutt, 1998). *ISO* now allows us to re-address this question. Examining the global luminosity of disks of spiral galaxies, Roussel et al. (1999b) establish a clear correlation between the MIR and Hα luminosity of *disks* (see fig. 1a). This correlation is linear and implies that in the disks of normal galaxies, the energy source for the MIR emission is the young stellar population and therefore that it can be used as a star formation tracer. There are however a few caveats: (1) in the disk of normal spirals, the broadband [6.75μm]/[15μm] color is ~ 1, as expected if there is little if any contribution from very small hot grains such as observed in HII regions (see sec. 1.2). This will not be the case in stronger star forming galaxies (see sec. 5). (2) The central regions of spiral galaxies typically have a lower [6.75μm]/[15μm] ratio (e.g. Sauvage et al., 1996; Roussel et al., 1999a; Dale et al., 1999), possibly indicating again a higher local star formation rate. Therefore, in the case of an unresolved galaxy, Roussel et al. (1999b) argue that their calibration should provide a lower limit to the actual star formation rate.

The possibility to separate the nuclear region from the disk of the galaxy in the MIR now allows a re-investigation of the FIR-Hα correlation. This correlation is known to be non-linear, implying that more than one process is present and that the FIR cannot be directly used to infer star-formation rates (e.g. Sauvage & Thuan, 1992). Roussel et al. (1999b) have selected in their sample those galaxies with the smallest contribution of the central region *in the MIR maps* and show that for this sample the FIR-Hα correlation is very good and linear (fig. 1b). This indicates that the non-linearity present in the general FIR-Hα relation is induced by the nuclear component and that in the disk of normal galaxies, the FIR emission collected by *IRAS* is mostly from dust heated by the young stellar population.

3. Starbursts in the infrared

As already mentioned in section 2.3, some galaxies have MIR colors that resemble those found in nearby HII regions (e.g. compare Dale et al., 1999, to Contursi et al., 1997). This indicates that the MIR-FIR properties of galaxies are useful tools to monitor star formation.

3.1. Spectral energy distributions of starburst galaxies

A first effect that can easily be understood is that the SED of a starburst galaxy is globally shifted toward higher dust temperatures. For instance, Krügel et al. (1998) found that the starburst galaxies they studied did not require a cold (10 K) dust phase in their SED. This is also confirmed by Klaas et al. (1999), or in NGC 6090 (Acosta-Pulido et al., 1999): the coldest dust phase required for these galaxies is 30-50 K, in sharp contrast with what is obtained on normal spirals (see sec. 2.1). One should however note that these temperature decompositions depend highly on the exponent of the dust emissivity assumed (β = 1-2): Klaas et al. (1999) note that if $\beta = 2$ were used for their sample, instead of $\beta = 1$, there would be room for a colder dust phase. Therefore, rather than attempting to determine precise temperature values, one should remember that in starburst galaxies, the peak of the SED shifts from 100-200 μm to the 60-100 μm range.

The shift in the FIR is obviously reflected in the MIR. As the heating intensity rises, the small grain emission gradually shifts towards short wavelengths in the MIR window (see section 1.2), producing a steeply rising continuum that can start anywhere in the 4-20 μm range. It is important to realize that the wavelength at which the small grain continuum dominates over the infrared bands can vary and *is in fact most of the time beyond 12 μm.* This can lead to some starburst galaxies being erroneously classified as normal from their *ISOPHOT*-S spectrum (e.g Lu et al., 1999), which only extends to 12 μm.

Observations of known starbursts in the MIR also reveal that the infrared bands are rarely suppressed: all the star-forming regions of the Antennae show significant, if not dominant, emission from the infrared bands (Vigroux et al., 1996); the sample of galaxies with warm *IRAS* colors selected by Mouri et al. (1998) shows well-defined infrared bands but no sign yet of a rising continuum. Finally, the template starburst spectrum used by Lutz et al. (1998) (again from *ISOPHOT*-S) is not markedly different from that of NGC 891 (Mattila et al., 1999). Therefore, the clear signature of a starburst-powered galaxy in the MIR spectrum is more the presence of a strong continuum longward of $\sim 12\,\mu$m than the absence of infrared bands (see e.g. Crowther et al., 1999 for a nice example on NGC 5253)

Finally, an important point for starburst galaxies is the amount of extinction present on the line of sight. Because infrared bands are located on both sides of the $9.7\,\mu$m silicate feature, a band-dominated extinction-free MIR spectrum will still show a depression around $10\,\mu$m. Optical depth measurements are thus better made with line ratios (Lutz et al., 1996) and, in starburst galaxies, span a very wide range, $A_V \sim$10-100 (Genzel et al., 1998). More recently an attempt to measure the extinction by its imprint on the infrared band shapes has met with some success (Rigopoulou et al., 2000) and confirmed the range mentioned above.

3.2. Star formation in high IR luminosity galaxies

A large amount of work has been devoted to the understanding of the physical processes at work in high IR luminosity objects, mostly interacting/merging systems. Although, as mentioned in Sanders (1999), 3-4 of the 5 closest examples of ultraluminous IR galaxies (ULIRGs) contain a powerful if not dominant AGN, most ISO studies on luminous IR galaxies emphasize the importance of the starburst process in the generation of the IR luminosity (but see sec. 5). A very interesting point comes from studies of luminous and ultraluminous IR galaxies (the frontier being located at $L_{8-1000\mu\mathrm{m}} = 10^{12}\,L_\odot$).

For their *ISOCAM* sample of Luminous IR galaxies (LIG), Hwang et al. (1999) show a clear anti-correlation between the compactness of the infrared source and the angular separation between the interacting objects. This seems at odds with the absence of any correlation in the MIR properties of ULIRGs with the angular separation (but note that little IR imaging is available for ULIRGs). Similarly, Gao & Solomon (1999) have shown that, in LIGs, there is a clear anti-correlation between the star formation efficiency (SFE) and the angular separation (i.e. higher SFE for closer pairs). No such correlation is seen in the ULIRG sample of Rigopoulou et al. (2000), but very interestingly, the maximum SFE reached by LIGs is of the order of the mean SFE of

ULIRGs. This seems to place ULIRGs as a limit-case for interaction triggered star-formation and may explain the lack of clear correlations with interaction parameters for the ULIRG sample. It also supports the conclusions of e.g. Genzel et al. (1998) and Rigopoulou et al. (2000) that the ULIRG phenomenon is mostly related to individual properties of the interacting galaxies and not directly to the interaction itself.

Of interest then are the spatially resolved observations of starburst galaxies and ULIRGs. A common point of these studies is the discovery that in many cases, a significant part of the luminosity is produced by very compact, mostly extranuclear, sources. This was first seen in the Antennae (Vigroux et al., 1996), but is now observed also in Mrk 171 (Gallais et al., 1999), NGC 253 (Keto et al., 1999), NGC 5253 (Crowther et al., 1999), or Arp 220 (Soifer et al., 1999). A plausible interpretation of these sources is that they are buried super-star-clusters, that will later evolve in the blue super-star clusters seen in interacting galaxies (e.g. O'Connel et al., 1994). Given the power output of these clusters, their infrared phase should be quite short, a fact that fits well in the scenario of starburst progression during the merging phase of interacting galaxies proposed by Rigopoulou et al. (2000).

3.3. The [CII] deficit

One of the most surprising findings of *ISO* comes from *ISOLWS*: Malhotra et al. (1997) observed that galaxies with the highest [60μm]/[100μm] or star formation activity exhibited lower-than-expected [CII]-to-FIR luminosity ratios. This was unexpected given that [CII] is predicted to be strong in regions exposed to far-UV photons that abonds in these galaxies. This deficit was later confirmed by Luhman et al. (1998) in a sample of ULIRGs. Reasons for this deficit are still unknown. Extinction or self-absorption have been rejected as the very large A_V required ($\sim$400-1000) are not confirmed by any other extinction measurements. Favored explanations are (1) a decreased efficiency of photoelectric heating in very high UV fields (grains become positively charged or are destroyed, thus reducing the number of photo-electrons), or (2) softer than expected UV radiation fields in ULIRGs due either to a troncated initial mass function or the presence of aging starburst regions.

4. Active galaxies

Our understanding of active galaxies has advanced greatly in the recent years, mainly through multiwavelength observations of these objects. The infrared plays a particular role in these studies, for three reasons:

- It is in the infrared that the spectra of these objects peak. Thus, a precise knowledge of the infrared flux is necessary to assess the bolometric luminosity, and the energetics of active galaxies.

- Multiwavelength observations of AGNs tend to support a unified scheme, according to which these objects are intrinsically similar, with various scales, but are viewed under different angles. An energy source in their center is surrounded by a torus of obscuring gas and dust, with a radius of parsecs to tens or a hundred parsecs. The observational properties of the objects depend not only of the energy source, but also on the angle at which they are observed with respect of the torus. In this scheme, radio quiet, steep spectrum quasars and Seyfert 1 galaxies are seen at intermediate angles, flat spectrum quasars and BL Lac are pole-on, and radio-galaxies and Seyfert 2 edge-on. In the infrared, it is possible to observe the direct emission of the torus. Models indicate that tori are still optically thick in the MIR (Pier & Krolik, 1993; Granato et al., 1997). But in the FIR a simple prediction of the unification models is that sources of similar energy should emit the same amount of thermal radiation from torus-heated dust.

- The infrared is a domain so rich in spectral lines (see fig. 2), less subject to absorption than the optical ones, that infrared spectra permit indirectly to determine the ionizing continuum.

4.1. Unification scheme and ISO observations

Many *ISOPHOT* results on quasars and radio-galaxies are still pending, but those available tend to support the unification scheme. For radio quiet and steep spectrum QSOs, the SED has a bump at around $60\,\mu$m, and declines beyond $100\,\mu$m, as expected for multi-temperature dust emission in the range of tens to hundreds of K (Haas et al., 1998). Most interestingly, the prototype radiogalaxy Cygnus A exhibits a similar SED; but 3C20, with a similar radio flux, is not seen by *ISOPHOT*. Also, on the whole, QSOs appear to be more luminous in the FIR than radio sources, thus, if the unification scheme is correct, the torus is also optically thick in the FIR. The SED of flat-spectrum QSOs is dominated by synchrotron emission, but for 3C279, a variable quasar, "the (dust) bump pryes above the synchrotron spectrum" when the overall emission is low (Haas et al., 1998). In the case of Seyfert galaxies, the synchrotron emission is weak or absent in the IR. In the course of a study with *ISOPHOT* of 10 CfA galaxies, Pérez Garcia et al. (1998) decompose the emission in two or three phases: warm (150 K, corresponding to the nucleus), cold (40 to 50 K, star forming regions), very cold (10 to 20 K, cirrus). As expected from the unification scheme, the warm phase is colder for Seyferts 2 than for Seyferts 1. The respective extensions of the cold and the warm component in the IR are similar to those of the cold and the hot component in the R band. But, in the FIR, the nuclear emission can be a substantial fraction of the total FIR, and thus of the total $L_{\rm bol}$ of the galaxy.

Clavel et al. (1998) did a statistical study with *ISOPHOT*-S encompassing 26 Seyfert 1 and 28 Seyfert 2 galaxies. They found that while Seyfert 2 exhibit a weak continuum and strong infrared bands, Seyfert 1 have 7 times stronger continua and weak or non-existing infrared bands. This also agrees with expectations from MIR optically thick torus models.

4.2. IR lines in Seyfert galaxies and the Big Blue Bump

With the spectrometers on board of *ISO*, complemented by *ISOPHOT*-S and the CVF of *ISOCAM*, it has been possible to obtain a wide variety of results on Seyfert infrared spectral properties. We display in fig. 2 the combined *ISOSWS*+*ISOLWS* spectrum of Circinus, a prototype Seyfert 2 at 4 Mpc (Moorwood, 1999). There are 30 fine structure lines in this spectrum, emitted by species with ionization energies in the 8 to 300 eV range. Note in particular the prominent high excitation lines of [OIV] and [NeV], mainly produced by the hard photons of AGNs. Detailed modeling allowed Moorwood et al. (1996) to derive from this spectrum the ionizing EUV continuum, assuming that clouds are ionization bounded. The result is a very hard ionizing continuum, with a very pronounced bump around 70 eV. This Big Blue Bump is required by accretion disk models (Laor, 1990), and can be considered the signature of a black hole. However, a similar derivation made by Sturm et al. (1999) on the Seyfert 1 NGC 4151, at 13 Mpc, concluded that in the EUV spectrum of this galaxy there is a void, rather than a bump, at 70 eV; they attribute this to absorption by neutral hydrogen placed between the narrow line region and the ionizing source.

4.3. Spectral characteristics of active galaxies

In addition to an active nucleus, Circinus is known to also have a circumnuclear starburst (Moorwood et al., 1996); salient features of its spectrum (fig. 2), apart from the large number of fine structure lines, are the presence of infrared bands, the continuum bump due to hot dust and the broad silicate absorption around 9.7 μm. In a subsequent study, using the *ISOCAM*-CVF, Moorwood (1999) showed that the infrared band emission does not originate in the starburst ring, but is in fact caused by the remnants of an earlier starburst episode.

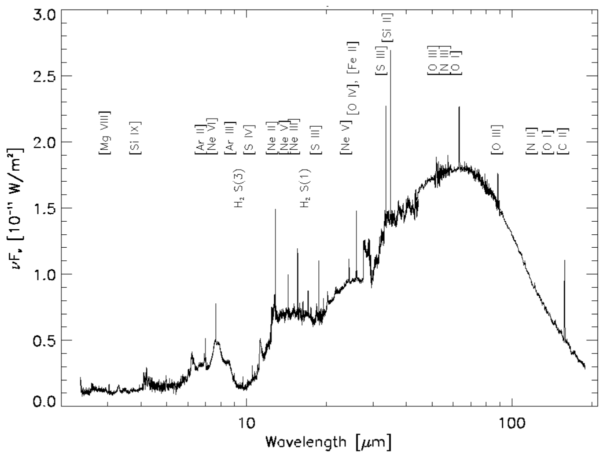

Figure 2. The combined *ISOSWS+ISOLWS* spectrum of the Circinus galaxy (from Moorwood 1999). Fine structure ionic lines as well as some H_2 rotational lines are labeled. Note also the infrared bands in the 6-15 μm range as well as the probable silicate absorption bands.

Another interesting case is that of Centaurus A, the closest active galaxy, at only 3.1 Mpc, which is suspected of hosting a misaligned BL LAC nucleus (e.g. Bailey et al., 1986) at the center of an elliptical galaxy. An *ISOCAM* map by Mirabel et al. (1999) reveals the presence of a bisymmetric structure, similar to that of a barred spiral galaxy, in the central region of the giant elliptical galaxy. This strange "galaxy" is composed of the tidal debris of small galaxies accreted by the elliptical galaxy in the last 10^9 years. Marconi et al. (2000) recently observed this object with *NICMOS*, on board *HST*, and found Paα emission indicative of enhanced star formation at the edges of the bar seen with *ISO*, probably due to shocks associated with the bar. The *ISOSWS* spectrum of Centaurus A (Alexander et al., 1999) is that of an AGN with a circumnuclear starburst, and has been modeled by these authors with a 3.6 pc torus inclined at 45°. *ISOCAM*-CVF spectra from 5 to 16 μm permit to distinguish very clearly between the nucleus dominated by a fast rising continuum, and the star formation regions emitting essentially in the infrared bands.

5. Mid-infrared diagnostics to identify the nature of galaxies

The first such tool is one that combines *ISO* and *IRAS* information in the so-called *ISO-IRAS* color diagram. It compares the [6.75μm]/[15μm] ratio from *ISOCAM* to the [60μm]/[100μm] ratio from *IRAS* (see fig. 3a). It is a first step in assessing the nature of *ISO* galaxies. For a large

Figure 3. (a-top left) The ISO-IRAS color diagram, that plots the [6.75μm]/[15μm] ratio versus the [60μm]/[100μm] ratio. Asterisks are for starburst and active galaxies, diamonds for Virgo spirals, filled circles for barred spirals and open squares for blue compact galaxies. (b-right) The Genzel et al. (1998) diagram that combines the [OIV]/[NeII] ratio with the 7.7 μm line-to-continuum ratio. AGN-dominated galaxies have small 7.7 μm L/C ratios and large [OIV]/[NeII] ratios. Known starburst are plotted as triangles, known AGNs as crossed squares and their sample of ULIRGs as filled circles. (c-bottom left) The Laurent et al. (2000) diagram for *ISOCAM* data, that plots the ratio of the 15 μm band to the 6.75 μm band versus the ratio of the 6.75 μm band to the 6 μm band. Galaxies from the *ISOCAM* central program are placed in that diagram. Large symbols represent objects with a known AGN that, expectedly, fall in the AGN corner of the diagram.

range of [60μm]/[100μm] colors, the [6.75μm]/[15μm] color is roughly constant. This is the space occupied by normal star forming galaxies. It is only beyond an *IRAS* color $\geq$-0.2 that the [6.75μm]/[15μm] color decreases. Only blue compact, interacting or starburst galaxies occupy that part of the diagram, an expected fact from the previous discussion: the radiation field is high enough that the small grain continuum has been shifted into the *ISOCAM* band.

This region of the *ISO-IRAS* color diagram is obviously of high interest as it hosts galaxies providing most of the IR energy collected in the Universe, and it has therefore been explored in more details. Genzel et al. (1998) were very succesful in arranging a sample of 13 ULIRGs on a plot representing the ratio [OIV]/[NeII] versus the relative strength of the 7.7 μm infrared band (fig. 3b). In this diagram, the ULIRGs tend to lie close to the starburst region, but some clearly contain an energetic AGN. Similar analyzes, using only the 7.7 μm line-to-continuum (L/C) tool on larger samples were presented by Lutz et al. (1998) and Rigopoulou et al. (2000) from which they conclude that indeed the fraction of ULIRGs powered by an AGN increases with the infrared luminosity, but also that ULIRGs are predominantly ($\sim$70-80%) starburst powered.

This 7.7 μm L/C tool is however ambiguous as some starbursts have no infrared bands while some AGN exhibit strong bands. Thus the Laurent et al. (2000) diagnostic (fig. 3c), working on the broader *ISOCAM* band, uses the flux ratio of the broad 6.75 μm to the broad 15 μm band compared to the flux ratio of the broad 6.75 μm band to the narrow 6 μm band to make a finer distinction between AGN, starburst and normal star-forming regions. Given that AGNs and starbursts have very different continuum shapes, this tool is very successful in distinguishing one from the other. Since AGNs have much more flux in the 6 μm range than starburst or star-forming galaxies, a "band-less" starburst is not mistaken for an AGN. Applying this tool to ULIRGs show that a fraction larger than that identified by e.g. Rigopoulou et al. (2000) is AGN-powered. This type of method has great potential for future studies with the NGST, if its wavelength range is sufficiently extended.

6. Deep surveys

Gains in sensitivity with *ISOCAM*, compared to *IRAS* at 12 μm, have made it possible to extend the range of MIR counts by three orders of magnitude. Similarly *ISOPHOT* allowed to perform, for the first time, surveys at 175 μm, a range of considerable cosmological interest. The ISO counts give a radically new view of star formation in the universe between now and $z \sim 2$.

6.1. MIR templates and K correction effects

ISOCAM surveys have essentially been performed in two filters, around 6.75 and 15 μm (but see also the 12 μm survey of Clements et al., 1999). Throughout this review, we have presented, discussed or alluded to template spectra of the various galaxy types in the MIR. For nearby objects, the 6.75 μm filter probes infrared bands, while the 15 μm filter probes preferentially warm dust and neon lines. As the redshift increases, the infrared bands are more and more shifted to the 15 μm filter. For galaxies intrinsically bright in these bands, the K correction at 15 μm is positive (sources appear to be fainter with increasing distances), but flat between $z \simeq 0.4$ and 1.3. For objects with $z > 0.4$, the 6.75 μm filter has access only to the starlight or to an eventual AGN contributions; the same is true at 15 μm if $z > 1.5$ (see Aussel et al., 1999a; Elbaz et al., 1999).

The situation is even more favorable for surveys with ISOPHOT at 175 μm; there, since most galaxy SEDs peak well below this wavelength, as z increases, the K correction is negative, favoring detection of distant galaxies.

6.2. The surveyed regions

The fields surveyed have been selected for their low zodiacal and cirrus emission; the second point is particularly important for the FIR studies. They can be found, in the Northern hemisphere, in the Lockman Hole, and in the Southern hemisphere, in the Marano field. Both fields have been the subject of multiwavelength studies, but often not to the depth required to interpret the results of *ISOCAM* surveys. These surveys are therefore well complemented by studies on well-known fields, the HDF North and a CFRS field at 6.75 and 15 μm, and the SSA13 field at

6.75 μm. Few results are available on the other fields at 6.75 μm, where observations at other wavebands, not yet available for many of the surveys, are crucial to avoid contamination by galactic stars (but see Taniguchi et al., 1997; Flores et al., 1999a; Sato et al., 1999), and for lack of space we concentrate here, for ISOCAM, on 15 μm results.

6.3. The nature of the ISOCAM 15 μm galaxies in a CFRS field and in HDF-North

Combining the deep survey on a CFRS field (Flores et al., 1999b) and that on the HDF North (Aussel et al., 1999a), 83 galaxies have been detected at 15 μm, with fluxes in excess of 250 μJy for the CFRS, and >100 μJy for the HDF. The positional accuracy of 6" allowed in almost all cases to identify an optical counterpart, brighter than I(Kron-Cousins)$\simeq$23; the mean redshift is 0.7.

In the CFRS field, Flores et al. derived the type of the galaxies for which they had enough spectral information, including radio fluxes, by comparing their SED to local templates compiled by Schmitt et al. (1997). They found that more than two thirds of these galaxies are starburst or post-starburst, and that at least at $z \sim 0.4$ to 0.6, their overall contribution to the global star formation rate is dominant.

Aussel et al., (1999a,b) compared the 27 MIR HDF sources with known redshift to a reference sample of HDF sources from an optical catalogue. While the redshift distribution of the two samples are similar, the color distributions are very different. *ISOCAM* picks up galaxies with B-I colors corresponding to spirals, and is blind to the faint blue population responsible for the excess in the B counts (Ellis, 1997). In summary: it appears that most of the MIR galaxies have luminosities of the order or brighter than $L_{\rm bol} \simeq 5\,10^{11}\,L_{\odot}$ (i.e. LIGs but not ULIGs), and are spiral or merging systems with normal colors, harboring an obscured starburst or a very well hidden active nucleus.

6.4. Source counts at 15 μm

Thanks to the *ISOCAM* surveys, it has been possible to extend by three orders of magnitude the $\log N - \log S$ diagram of MIR sources with respect to the IRAS results. Fig. 4, from Elbaz et al. (1999), shows the integral and the differential counts derived from the Lockman Hole and the Marano shallow, deep and ultra-deep surveys performed on guaranteed time (IGTES, PI C.Cesarsky), the two HDF surveys, and an extension to fainter fluxes through the study of a lensed galaxy cluster Altieri et al. (1999). These counts are complemented, at flux >2 mJy, by the results of ELAIS (PI M. Rowan Robinson; see Serjeant et al., 2000). Five independent surveys confirm the breaks of these curves at

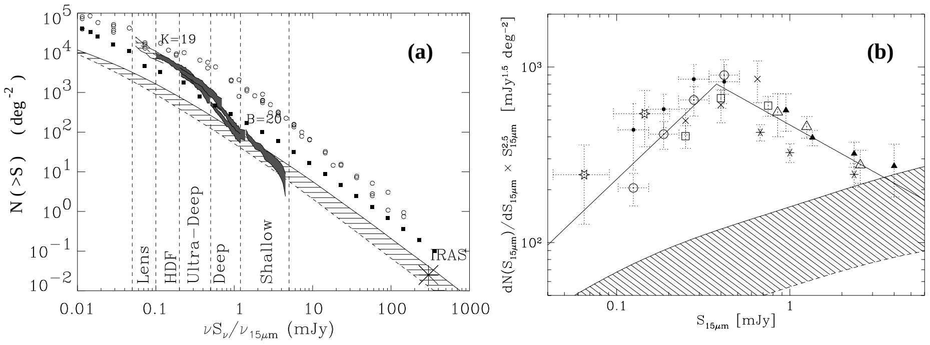

Figure 4. (a-left) A summary plot of the integral counts of *ISOCAM* 15 μm surveys with 68% confidence contours. K counts (Gardner et al., 1993) and B counts (Metcalfe et al., 1995), multiplied by $\nu/\nu_{15}\mu$m to represent the relative energy densities at high fluxes are overplotted with circles and filled squares, respectively. The hatched area materializes expectations from models assuming no evolution and normalized to the IRAS 12 μm local luminosity function (see Elbaz et al., 1999 for details). (b-right) Differential number counts of 15 μm galaxies (also from Elbaz et al. 1999). The counts are normalized to an euclidian distribution of non-evolving sources which would have a slope of $\alpha = -2.5$ in such a universe. The hatched area has the same meaning as in (a).

400 μJy; in the differential plot, the slope passes from (-1.6) to (-3) for faint sources. On the same figures are shown the expectations from models assuming no evolution, which take into account the infrared bands in the galaxy spectra. Despite the uncertainties in these curves (see discussion in Elbaz et al., 2000), there is no question that at least at fluxes below 400 μJy, these source counts imply strong evolution in the population of MIR sources.

The *ISOCAM* counts also indicate that the sources responsible for them are not ULIRGs with spectra like Arp 220; otherwise, they would produce an infrared background at 140 μm in excess of the value observed by *COBE* (Puget et al., 1996).

6.5. Source counts at 175 μm

Deep counts with *ISOPHOT* at 175 μm in the Lockman Hole and in the Marano field (Kawara et al., 1999; Puget et al., 1999), down to 120 mJy, also give a $\log N - \log S$ curve with a steep slope and a source density which is higher by a factor of order 10 than extrapolations from *IRAS* or predictions of no evolution models. For these sources, identifications are uncertain, given the large error boxes. Because of the large negative K correction at this wavelength, it is likely that some of the sources seen are at z in the range 1 to 2. Indeed, using the *ISOCAM* results, one can show that they cannot be a population of galaxies with average redshift 0.7 and a spectrum like M 82 or Arp 220, since in that case *ISOCAM* would see many more sources in the range >1 mJy (Elbaz et al., 2000). Thus, while a fraction of the sources are in common, on the average *ISOCAM* and *ISOPHOT* sample different populations of sources. While *ISOCAM* pinpoints those of the B and K sources, at $z < 1$, that harbor activity hidden by dust, *ISOPHOT* misses many of them but can find more distant far-infrared beacons.

A conclusion on such a broad subject is hard to write, when a large number of our colleagues are devoting most of their time to a finer analysis of the *ISO* data. Let us instead remark that the areas where new infrared data turn out to be of key importance are growing day by day, strongly supporting future infrared missions.

Acknowledgements

We are grateful to the organizers for exerting the right pressure resulting in the timely delivery of the manuscript, and to the conference sponsors, the Anglo-American Chairman's fund and SASSOL, for allowing this very interesting meeting to take place.

References

Acosta-Pulido, J. A., Klaas, U. and Laureijs, R.: 1999, in The Universe as seen by ISO, Eds. P. Cox and M. Kessler, (ESA - SP 427:Paris), pp 849-851
Alexander, D. M., Efstathiou, A., Hough, J. H., et al.: 1999, in The universe as seen by ISO, Eds. M. F. Kessler and P. Cox, (ESA:Paris), pp 853-856
Altieri, B., Metcalfe, L., Kneib, J. P., et al.: 1999, *A&A*, **343**, pp L65-L69
Alton, P. B., Bianchi, S., Rand, R. J., et al.: 1998a, *ApJ*, **507**, pp L125-L129
Alton, P. B., Trewhella, M., Davies, J. L., et al.: 1998b, *A&A*, **335**, pp 807-822
Aussel, H., Cesarsky, C. J., Elbaz, D. and Starck, J. L.: 1999a, *A&A*, **342**, pp 313-336
Aussel, H., Elbaz, D., Cesarsky, C. J. and Starck, J. L.: 1999b, in The Universe as seen by ISO, Eds. P. Cox and M. Kessler, (ESA - SP 427:Paris), pp 1023-1026
Bailey, J., Sparks, W. B., Hough, J. H. and Axon, D. J.: 1986, *Nature*, **322**, pp 150
Bianchi, S., Alton, P. B., Davies, J. I. and Trewhella, M.: 1998, *MNRAS*, **298**, pp L49-L54
Boulanger, F., Abergel, A., Bernard, J. P., et al.: 1998a, in Star formation with the infrared space observatory (ISO), Eds. J. L. Yun and R. Liseau, (ASP conference series:Lisbon), pp 15-23
Boulanger, F., Boissel, P., Cesarsky, D. and Ryter, C.: 1998b, *A&A*, **339**, pp 194-200
Boulanger, F., Reach, W. T., Abergel, A., et al.: 1996, *A&A*, **315**, pp L325-L328
Cesarsky, D., Lequeux, J., Abergel, A., et al.: 1996, *A&A*, **315**, pp L309-L312
Clavel, J., Schultz, B., Altieri, B., et al.: 1998, *to appear in* structure and kinematics of quasar broad line regions, Eds. C. M. Gaskell, W. N. Brandt, M. Dietrich and D. Dultzin-Hacyan, PASP conference series

Clements, D. L., Desert, F. X., Franceschini, A., et al.: 1999, *A&A*, **346**, pp 383-391
Colbert, J. W., Malkan, M. A., Clegg, P. E., et al.: 1999, *ApJ*, **511**, pp 721-729
Contursi, A., Lequeux, J., Hanus, M., et al.: 1997, *A&A*, **336**, pp 662-666
Cox, P., Roelfsema, P. R., Baluteau, J. P., et al.: 1999, in The Universe as seen by ISO, Eds. P. Cox and M. Kessler, (ESA - SP 427:Paris), pp 631-637
Crowther, P. A., Beck, S. C., Willis, A. J., et al.: 1999, *MNRAS*, **304**, pp 654-668
Dale, D. A., Helou, G., Silbermann, N. A., et al.: 1999, *AJ*, **in press**
Davies, J. I., Alton, P., Trewhella, M., et al.: 1999, *MNRAS*, **304**, pp 495-500
Devereux, N. A. and Young, J. S.: 1990, *ApJ*, **359**, pp 42-56
Elbaz, D., Cesarsky, C., Fadda, D., et al.: 1999, *A&A*, **submitted**
Elbaz, D., et al.: 2000, **in preparation**
Ellis, R. B.: 1997, *ARA&A*, **35**, pp 389
Flores, H., Hammer, F., Desert, F. X., et al.: 1999a, *A&A*, **343**, pp 389-398
Flores, H., Hammer, F., Thuan, T. X., et al.: 1999b, *ApJ*, **517**, pp 148-167
Gallais, P., Laurent, O., Charmandaris, V., et al.: 1999, in The Universe as seen by ISO, Eds. P. Cox and M. F. Kessler, (ESA - SP 427:Paris), pp 881-884
Gao, Y. and Solomon, P. M.: 1999, *ApJLett*, **512**, pp L99-L103
Gardner, J. P., Cowie, L. L. and Wainscoat, R. J.: 1993, *ApJLett*, **415**, pp L9-L12
Genzel, R., Lutz, D., Sturm, E., et al.: 1998, *ApJ*, **498**, pp 579-605
Granato, G. L., Danese, L. and Franceschini, A.: 1997, *ApJ*, **486**, pp 147-159
Haas, M., Chini, R., Meisenheimer, K., et al.: 1998, *ApJLett*, **503**, pp L109-L113
Haas, M., Lemke, D., Stickel, M., et al.: 1998, *A&A*, **338**, pp L33-L36
Hwang, C. Y., Lo, K. Y., Gao, Y., et al.: 1999, *ApJLett*, **511**, pp L17-L20
Israel, F. P., van der Werf, P. P. and Tilanus, R. P. J.: 1999, *A&A*, **344**, pp L83-L86
Kawara, K., Sato, Y., Matsuhara, H., et al.: 1999, in The Universe as seen by ISO, Eds. P. Cox and M. Kessler, (ESA - SP 427:Paris), pp 1017-1018
Kennicutt, R. C.: 1998, *ARA&A*, **36**, pp 189-231
Keto, E., Hora, J. L., Fazio, G. G., et al.: 1999, *ApJ*, **518**, pp 183-189
Klaas, U., Haas, M. and Schultz, B.: 1999, in The Universe as seen by ISO, Eds. P. Cox and M. Kessler, (ESA - SP 427:Paris), pp 901-903
Krügel, E., Siebenmorgen, R., Zota, V. and Chini, R.: 1998, *A&A*, **331**, pp L9-L12
Laor, A.: 1990, *MNRAS*, **246**, pp 369-383
Laurent, O., Mirabel, I. F., Charmandaris, V., et al.: 2000, *A&A*, **submitted**
Leger, A., d'Hendecourt, L. and Defourneau, D.: 1989, *A&A*, **216**, pp 148-164
Lu, N. Y., Helou, G., Silbermann, N., et al.: 1999, in The universe as seen by ISO, Eds. P. Cox and M. F. Kessler, (ESA - SP 427:Paris), pp 929-932
Luhman, M. L., Satyapal, S., Fischer, J., et al.: 1998, *ApJLett*, **504**, pp L11-L15
Lutz, D., Feuchtgruber, H., Genzel, R., et al.: 1996, *A&A*, **315**, pp L269-L272
Lutz, D., Spoon, H. W. W., Rigopoulou, D., et al.: 1998, *ApJ*, **505**, pp L103-L107
Malhotra, S., Helou, G., Van Buren, D., et al.: 1996, *A&A*, **315**, pp L161-L164
Malhotra, S., Helou, G., Stacey, G., et al.: 1997, *ApJLett*, **491**, pp L27-L30
Marconi, A., Schreier, E. J., Koekemoer, A., et al.: 2000, *ApJ*, **in press**
Mattila, K., Lehtinen, K. and Lemke, D.: 1999, *A&A*, **342**, pp 643-654
Metcalfe, N., Shanks, T., Fong, R. and Roche, N.: 1995, *MNRAS*, **273**, pp 257-276
Mirabel, I. F., Laurent, O., Sanders, D. B., et al.: 1999, *A&A*, **341**, pp 667-674
Moorwood, A. F. M.: 1999, in The universe as seen by ISO, Eds. P. Cox and M. F. Kessler, (ESA - SP 427:Paris), pp 825-831
Moorwood, A. F. M., Lutz, D., Oliva, E., et al.: 1996, *A&A*, **315**, pp L109-L112
Mouri, H., Taniguchi, Y., Sato, Y. and Kawara, K.: 1998, *A&A*, **334**, pp 482-488
O'Connel, R. W., Gallagher, J. S. and Hunter, D. A.: 1994, *ApJ*, **433**, pp 65-79
Pagani, L., Lequeux, J., Cesarsky, D., et al.: 1999, *A&A*, **submitted**

Perez Garcia, A. M., Rodriguez Espinosa, J. M. and Santolaya Rey, A. E.: 1998, *ApJ*, **500**, pp 685-692

Pier, E. A. and Krolik, J. H.: 1993, *ApJ*, **418**, pp 673-686

Puget, J. L., Abergel, A., Bernard, J. P., et al.: 1996, *A&A*, **308**, pp L5-L8

Puget, J. L., Lagache, G., Clements, D. L., et al.: 1999, *A&A*, **345**, pp 29-35

Rigopoulou, D., Spoon, H. W. W., Genzel, R., et al.: 2000, *AJ*, **in press**

Roussel, H., Vigroux, L., Sauvage, M., et al.: 1999a, in The Universe as seen by ISO, Eds. P. Cox and M. Kessler, (ESA - SP 427:Paris), pp 957-960

Roussel, H., Sauvage, M. and Vigroux, L.: 1999b, *A&A*, **submitted**

Sanders, D. B.: 1999, *to appear in* Ultraluminous Galaxies: Monsters or Babies?, Ringberg Castle Conference

Sato, Y., Cowie, L. L., Taniguchi, Y., et al.: 1999, in The Universe as seen by ISO, Eds. P. Cox and M. Kessler, (ESA - SP 427:Paris), pp 1055-1058

Sauvage, M., Blommaert, J., Boulanger, F., et al.: 1996, *A&A*, **315**, pp L89-L92

Sauvage, M. and Thuan, T. X.: 1992, *ApJLett*, **396**, pp L69-L73

Schmitt, H. R., Kinney, A. L., Calzetti, D. and Storchi-Bergmann, T.: 1997, *AJ*, **114**, pp 592-612

Serjeant, S., et al.: 2000, *MNRAS*, **submitted**

Smith, B. J.: 1998, *ApJ*, **500**, pp 181-187

Soifer, B. T., Neugebauer, G., Matthews, K., et al.: 1999, *ApJ*, **513**, pp 207-214

Sturm, E., Alexander, T., Lutz, D., et al.: 1999, *ApJ*, **512**, pp 197-203

Taniguchi, Y., Cowie, L. L., Sato, Y., et al.: 1997, *A&A*, **328**, pp L9-L12

Verstraete, L., Puget, J. L., Falgarone, E., et al.: 1996, *A&A*, **315**, pp L337-L340

Vigroux, L., Mirabel, F., Altieri, B., et al.: 1996, *A&A*, **315**, pp L93-L97